IEEE Access
Multidisciplinary | Rapid Review | Open Access Journal

Digital Object Identifier

Deep Learning-based Automatic Modulation Classification with Blind OFDM Parameter Estimation

MYUNG CHUL PARK[1], DONG SEOG HAN[1] (Senior Member, IEEE)
[1]School of Electronic and Electrical Engineering, Kyungpook National University, 80 Daehak-ro, Buk-gu, Daegu 41566, Korea

Corresponding author: Dong Seog Han (e-mail: dshan@knu.ac.kr).

This research was supported by Basic Science Research Program through the National Research Foundation of Korea (NRF) funded by the Ministry of Education (2021R1A6A1A03043144).

ABSTRACT Automatic modulation classification (AMC) is an essential factor in dynamic spectrum access to fulfill the spectrum demand of 5G wireless communications for achieving high data rate and low latency. Many deep learning (DL)-based AMC methods have achieved improved accuracy performance for classifying analog modulation schemes, single-carrier-based modulation schemes, and multi-carrier signals using several DL architectures such as the convolutional neural network (CNN) and long-short term memory (LSTM). However, most conventional DL-based AMC methods have confused the orthogonal frequency multiplexing division (OFDM)-based signals with different OFDM useful symbol lengths. To resolve the issue, we propose a CNN model operating on the fast Fourier transformation window banks (FWB) to extract the useful symbol length in OFDM, which represent the identification of each OFDM-based wireless communication technology. After extracting the OFDM useful symbol length, we propose a DL-based AMC system combined with FWB and in-phase and quadrature phase (IQ) signals to classify the OFDM symbol length and single-carrier modulation schemes simultaneously. Furthermore, we explore the constraints of the FWB parameters according to the length and the FFT size of the OFDM signal to achieve good classification accuracy through the experiment. We constructed a dataset by generating OFDM signals of different lengths while changing the FFT size in a fixed bandwidth and by selecting only quadrature amplitude modulation (QAM) schemes from RadioML2016.10a. Experimental results show the improved performance of the classification accuracy by about 30% over conventional classifiers in additive white Gaussian noise, synchronization impairments, and fading environments.

INDEX TERMS Automatic modulation classification, Cognitive radio, deep learning, modulation, neural networks, Orthogonal frequency-division multiplexing (OFDM)

I. INTRODUCTION

THE fifth generation (5G) wireless communication system is an attractive technology to achieve high performance in terms of high data rate and low latency. The efficient spectrum use needs to overcome the increased spectrum requirements for achieving large capacity. The dynamic spectrum access (DSA) technology improves the spectrum efficiency by sensing a used spectrum. Understanding the sensing signal in the spectrum is essential to determine the validation of the signal for the spectrum accessibility. To address the issue, automatic modulation classification (AMC) is a crucial factor to identify the spectrum utility by classifying the modulation type of the signal.

The conventional statistical-based approaches for AMC extract hand-crafted expert features such as cyclostationarity, spectral correlation function (SCF), and higher-order statistics (HOS) to classify modulation types [1]–[3]. The expert features identify the signal type by finding repeated fundamental frequencies [4], [5]. Therefore, the machine learning techniques, such as support vector machine (SVM) and k-nearest neighbor (KNN), classify the modulation schemes using a combination of the extracted features [6]. However, the aforementioned methods degrade the classification accuracy due to the dynamic channel environment [7].

Recently, many deep learning (DL)-based AMC schemes have been proposed to improve the classification accuracy in the dynamic channel using the raw time-series in-phase & quadrature phase (IQ) signals without hand-crafted expert features. O'Shea *et al.* [8] proposed a convolutional neural network (CNN) structure to extract features from the IQ

signals for classifying the modulation schemes. Rajendran *et al.* [9] proposed long-short term memory (LSTM)-based AMC systems [10] to reduce the complexity. Peng *et al.* [11] proposed a constellation diagram (CD) to transform a time-series IQ signal into an image for adopting AlexNet [12] and GoogLeNet [13] which have a powerful performance of classifying images. Zhou *et al.* [14] proposed slotted-CD imaging with characterizing the time-varying channel. Furthermore, they proposed the classifier consists of multiple CNNs in the first part, and a bidirectional LSTM (BiLSTM) and a deep neural network (DNN) in the other two parts, referred to as multiple CNN based BiLSTM and DNN (MCBLDN). Peihan *et al.* [15] proposed a waveform-spectrum multimodal fusion (WSMF) method that extracts features from multiple information using ResNet. The aforementioned DL-based AMC systems have improved performance for classifying between single-carrier-based modulation classification and multi-carrier signals.

The modern advanced wireless communication technologies adopt the orthogonal frequency division multiplexing (OFDM) signal transmitting information with multi-carrier. The OFDM-based wireless communication technologies have adopted quadrature amplitude modulation (QAM) schemes for the modulation scheme of subcarriers, and the overlapped modulation schemes between each technology make it difficult to distinguish each wireless communication technology. Therefore, to identify each technology, it is necessary to use a characteristic that each technology has a different own OFDM useful symbol length (same as the inverse of subcarrier spacing), not the modulation scheme. Rajendran *et al.* [9] have shown the limitation of DL-based AMC confusing on the OFDM-based signals between long-term evolution (LTE) and digital video broadcasting (DVB) in the Electrosense dataset [16].

To resolve the issue, we propose a CNN-based AMC using a fast Fourier transform window banks (FWB) to identify the OFDM-based wireless communication technology with different OFDM useful symbol lengths. Furthermore, we analyze the classification performance of the proposed system according to the OFDM useful symbol length and fast Fourier transform (FFT) size and achieve high classification accuracy by determining the optimal FWB parameters. Finally, we propose a CNN model that operates on the time-domain IQ data and FWB for classifying single carrier modulation schemes and the OFDM useful symbol length at the same time. Furthermore, we explore the proposed model performance for various signal-to-noise ratios (SNRs) under synchronization impairments and fading environments.

The rest of the paper is organized as follows. Section II briefly introduces the conventional statistical and DL approaches for classifying signal modulation and identifying OFDM parameters. Section III describes the system model. Section IV introduces the basic DL structure with IQ or amplitude and phase features and then proposes the FWB schemes to extract the OFDM useful symbol length feature on CNN. Section V overviews the single-carrier-based modulation dataset and the OFDM dataset for training and testing the networks. Section VI explains the classification results and discusses the limitation of the proposed model. Section VII presents conclusions and future work.

II. RELATED WORK

Conventional statistical AMC techniques are largely divided into likelihood-based (LB) and feature-based (FB) techniques. The LB scheme classifies a transmitted modulation scheme by calculating a coincidence probability according to each modulation scheme. Jefferson *et al.* [17] proposed a system that determines the modulation scheme with the highest cost by calculating the likelihood function of all modulation schemes in the candidate group and the received signal. The FB technique extracts higher-order cumulants (HOC) and analyzed the features for each modulation scheme [5]. As a decision method, the modulation method is predicted by applying machine learning techniques such as SVM [6]. Wenwu *et al.* [18] improves classification performance by constructing a deep belief neural network (DBN) based on a new feature parameter as the sixth-order cumulants of the extracted signal. Kim *et al.* [19] proposed a DBN-based AMC system with various HOCs features to improve classification performance and Lee *et al.* [20] analyzed the classification performance using the DBN-AMC system in a dynamic channel environment by selecting features robust to a fading environment. However, the aforementioned methods deteriorate the performance in complex channel environments [21].

The conventional technique for OFDM subcarrier spacing estimation uses autocorrelation with the cyclic prefix (CP) to extract the useful symbol and CP lengths. Peng *et al.* [22] estimate the OFDM useful symbol length by calculating the likelihood between the CP and the valid symbol. Punchihewa *et al.* [23] estimate the OFDM useful symbol period, symbol period, guard interval, and carrier frequency offset using the second order cyclostationary test. Bouzegzi *et al.* [24] extract the subcarrier spacing by using the cyclostationary characteristic. The CP length was estimated by using the correlation between the CP and the useful OFDM data symbol, but the performance deteriorates due to the distortion of the received signal by the fading channel and synchronization between the local oscillator (LO) of the transceiver [25]. To resolve the issue, many researches have conducted using cyclostationarity to estimate the channel response [26] and synchronization offset [27]–[29].

To solve the performance degradation due to channel characteristics and synchronization, O'Shea [30] proposed a method of classifying modulation schemes by extracting features through CNN using time-domain IQ signals. Furthermore, West and O'Shea [8] proposed VGG [31]-based one-dimensional CNN and ResNet to achieve remarkably improved performance. Rajendran *et al.* [9] proposed an AMC system using LSTM from CNN-LSTM [10] with the inputs of amplitude and phase (AP) instead of IQ signal, which overcomes the shortcoming of the CNN-LSTM with a large

amount of computation for applying low-end sensors. The LSTM-based AMC improves the accuracy performance even in the unmatched sampling rate environment. Hu *et al.* [21] proposed a robust modulation classifier in an uncertain noise channel environment by adopting the attention mechanism to the output of an LSTM layer. To compensate for the fading channel characteristics, Teng *et al.* [32] proposed a CNN technique to estimate the channel response for improving modulation classification using the accumulated amplitude and phase data.

Meng *et al.* [33] proposed an end-to-end trainable AMC system based on CNN by approximate the maximum likelihood (ML)-AMC with minimal performance loss and a two-step training method using 9-HOC features for fine-tuning. Peihan *et al.* [15] proposed a DL-based AMC system that extracts features by utilizing various input information such as IQ, AP, and FFT magnitude into ResNet, and classified modulation methods through DenseNet. Yashashwi *et al.* [34] proposed a correction module (CM)-CNN system that applies a correction module with CNN for estimating and compensating the synchronization offset and improved performance in an inconsistent synchronization environment. Shiyao *et al.* [35] proposed a generative adversarial network (GAN)-based AMC structure on improving the classification accuracy with data augmentation. Kulin *et al.* [36] proposed an end-to-end DL-based AMC system from data collection for classification. They analyzed the classification accuracy of the CNN-based AMC according to input information such as IQ, AP, and FFT magnitude. Zhou *et al.* [37] investigated and organized DL-based AMC techniques according to the characteristics of each system. To verify the classification performance of CNN in real environments, they demonstrated it using USRP and Pluto [38].

Peng *et al.* [11] proposed a method of transforming signals into a CD image to apply VGG, AlexNet, and GoogLeNet, which are excellent for image classification. Zhou *et al.* [14] improved the classification accuracy of AlexNet and GoogLeNet by adopting the proposed slotted-CD imaging technique to adapt to the time-varying channel characteristics. Wang *et al.* [39] proposed a sequential double CNN structure with an additional CD-input CNN structure to improve the classification performance of the highly confusing QAM types using IQ signals.

To classify multi-carrier signals and single-carrier signals, Mendis *et al.* [40] proposed a DBN system with the spectral correlation function (SCF) characteristics. Cheng *et al.* [41] improved the spectrum sensing performance of OFDM signals by inputting the time and frequency domain signals to the stacked autoencoder (SAE)-based DNN structure. Hong *et al.* [42] proposed a system for classifying modulation schemes transmitted by subcarriers of OFDM signals by applying parametric Relu (pReLU) to LeNet [30]. However, the DL-AMC schemes did not consider the OFDM-based signal with different lengths such as DVB and LTE, which are confused as shown in the Electrosense dataset [9].

III. SYSTEM MODEL

A wireless communication system transmits a signal to a receiver through a wireless channel environment as shown in Fig. 1. This section describes the transmitter, the radio channel model, and the receiver. And we overview the differences in the process of the single carrier modulator and OFDM signals in the transceiver.

A. TRANSMITTER

A transmitter transforms bit information streams into data symbols representing the modulation constellation point composed of IQ samples in the modulator processor. The data symbols transmit with single-carrier in time-domain after filtering with pulse shaping. The OFDM signal converts the symbols from time-domain to frequency-domain using the serial-to-parallel (S/P) converter. An inverse fast Fourier transform (IFFT) digital signal processing performs on the frequency-domain subcarriers to generate the OFDM symbol in the time domain. Then, the guard interval is inserted in front of each OFDM symbol to avoid inter-symbol interference (ISI) caused by multipath in the wireless radio channel. The cyclic prefix (CP), which extends the OFDM symbol cyclically to eliminate inter-carrier interference (ICI), is essentially an identical copy of the last portion of the OFDM symbol appended in the guard interval. In this system model, the transmitted signal $s(t)$ is as follows:

$$s(t) = \sqrt{E_s} \sum_{n} \sum_{k=0}^{K-1} x_{n,k} e^{\frac{j2\pi k(t-DT_c-nT_s)}{KT_c}} p(t-nT_s) \tag{1}$$

where the factor $\sqrt{E_s}$ is the aim of normalizing the signal power to make an average power spectral density (PSD) constantly. The factor $\sqrt{E_s}$ is determined by the modulation order L of QAM and the FFT size K as $E_s = 1/(KE_{QAM}) = 1/(K2E\{\mathfrak{Re}|x_{L-QAM}|^2\}) = 3/(2K(L-1))$. $x_{n,k}$ is the complex symbol sequence at the kth subcarrier in nth OFDM symbol. K is the number of subcarriers and $1/T_c$ is the transmission sampling rate f_s. The OFDM useful symbol length T_u is equal to KT_c and the subcarrier spacing is equal to $1/KT_c$. The length of the guard interval or cyclic prefix is set to DT_c. The symbol duration T_s is $T_s = (K+D)T_c$ in case of OFDM and is $T_s = T_c$ in case of single carrier. The pulse-shaping filter $p(t)$ is the root raised cosine (RRC) pulse with the roll-off factor α assuming unitary energy in case of the single carrier and is rectangular pulse shape in case of the OFDM.

The OFDM-based wireless communication technology has its own OFDM useful symbol length for each technology: e.g., 66.7 μs for LTE, 448 μs for DVB, 3.2 μs for WLAN, 12.8 μs for WiFi6, 66.67 μs, 33.33 μs, 16.67 μs, or 8.33 μs for 5G. To obtain a similar situation, assuming the same bandwidth for transmitting all signals, we generate OFDM signals with different lengths using different FFT sizes.

This article has been accepted for publication in a future issue of this journal, but has not been fully edited. Content may change prior to final publication. Citation information: DOI 10.1109/ACCESS.2021.3102223, IEEE Access

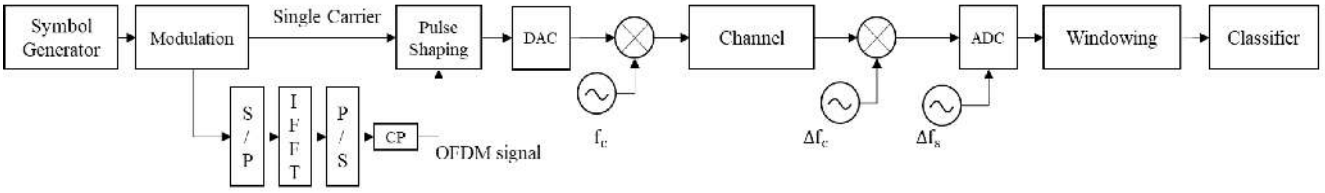

FIGURE 1. The system for dataset signal generation of automatic modulation classification system.

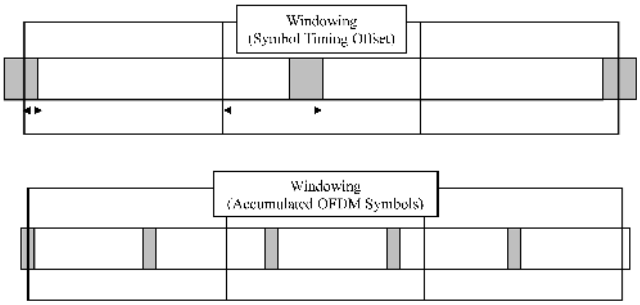

FIGURE 2. The symbol timing offset in receiver system for demodulating the transmitted OFDM signal.

B. WIRELESS CHANNEL

A radio wave signal reaches a receiver by two or more paths in a wireless communication system due to multipath which is the propagation phenomenon caused by reflection due to buildings or terrestrial objects. The multipath interference causes fading phenomenon occurred by destructive interference and phase distortion of the received signal. This multipath is modeled by a finite impulse response (FIR) filter as follows:

$$h(t) = \sum_{i=0}^{l} \beta_i \delta(t - \tau_i) \tag{2}$$

where $h(t)$ is the channel impulse response. β_i and τ_i are the gain and the delay time of the ith path respectively. l is the total number of multipath.

C. RECEIVER

The receiver transforms the received signal from the received antenna to a base-band signal by multiplying the signal's center frequency. At this time, the transformed signal is distorted by a frequency offset caused by a difference between the local oscillator (LO) of the transmitter and the receiver. In the sampling process, timing drift occurs by the mismatched sampling frequency of the LO in the analog-to-digital converter (ADC). The received signal $r(t)$ is modeled as

$$r(t) = \{s(t) * h(t)\} e^{j2\pi\Delta f_c t + \varphi(t)} + n(t) \tag{3}$$

where $n(t)$ is the additive Gaussian white noise (AWGN) which is caused by the electronic components in the receiver. Δf_c is the center frequency offset between transmitter and receiver LO, and $\varphi(t)$ is the phase offset which is caused by the timing drift Δf_s of sampling LO and mismatched symbol timing synchronization.

In order to demodulate the received signal, the receiver needs to know the modulation method of the transmission symbol to map the received symbol information to bit information. For this reason, the receiver needs a module that classifies the transmitted modulation scheme. The FFT processor is required since the OFDM signal transmits symbols in the frequency domain, unlike the single-carrier-based signal transmitting symbols in the time domain. At this time, the guard interval of the OFDM signal should be excluded to acquire the accurate constellation of the subcarrier. However, the FFT processor of the receiver occurs distortion of the received signal since the receiver does not know the guard interval and the useful data symbol lengths representing the start point of the useful data symbols as shown in Fig. 2. In addition, the magnitude of FFT output is increased by the situation in which several OFDM symbols enter one FFT input due to the mismatched length of the FFT window. Even though it is difficult to distinguish the OFDM useful symbol length in those effects, we try to classify the transmitted OFDM useful symbol length using deep learning without the conventional statistical process.

IV. SIGNAL CLASSIFICATION MODELS

The receiver classifies the modulation method of the transmission signal based on the received signal. In this section, we overview the characteristics of the signals used in the conventional classifier. Furthermore, we propose a CNN model operating on FWB to extract features of different subcarrier spacing.

A. BASELINE MODEL

The conventional DL-base AMC methods classify the modulation schemes as the single-carrier signal and multi-carrier signals as shown in Fig. 5. However, blind OFDM parameter estimation is required to identify the OFDM-based wireless communication technologies. Our statistical baseline model is based on the cyclostationarity test to estimate the OFDM useful symbol length [23]. The OFDM signal has second-order cyclostationarity at zero cyclic frequency (CF) and at a delay of the OFDM useful symbol length. The magnitude of cyclic autocorrelation (CAF) is calculated according to the candidate delay at zero CF ($\alpha = 0$) as follows:

This article has been accepted for publication in a future issue of this journal, but has not been fully edited. Content may change prior to final publication. Citation information: DOI 10.1109/ACCESS.2021.3102223, IEEE Access

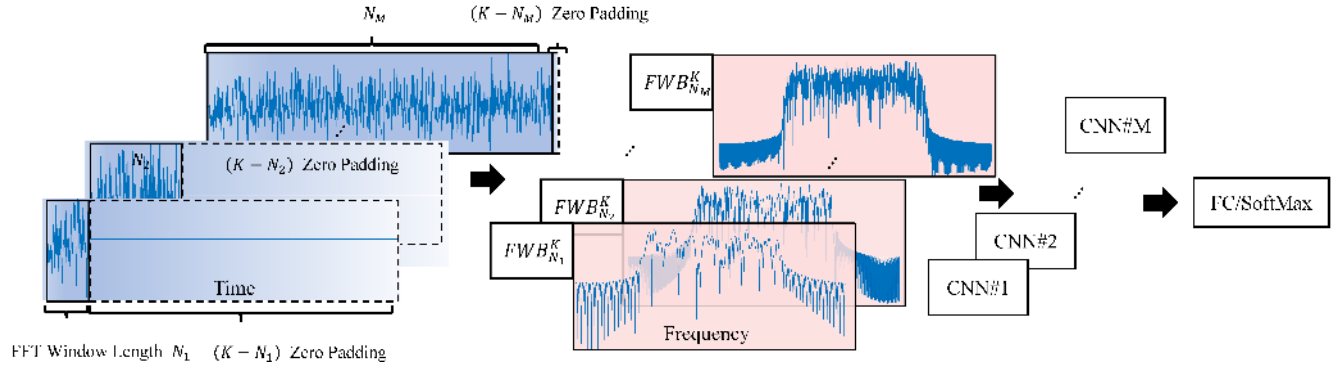

FIGURE 3. The proposed FFT Window bank (FWB) system for classifying different OFDM-based wireless communication systems.

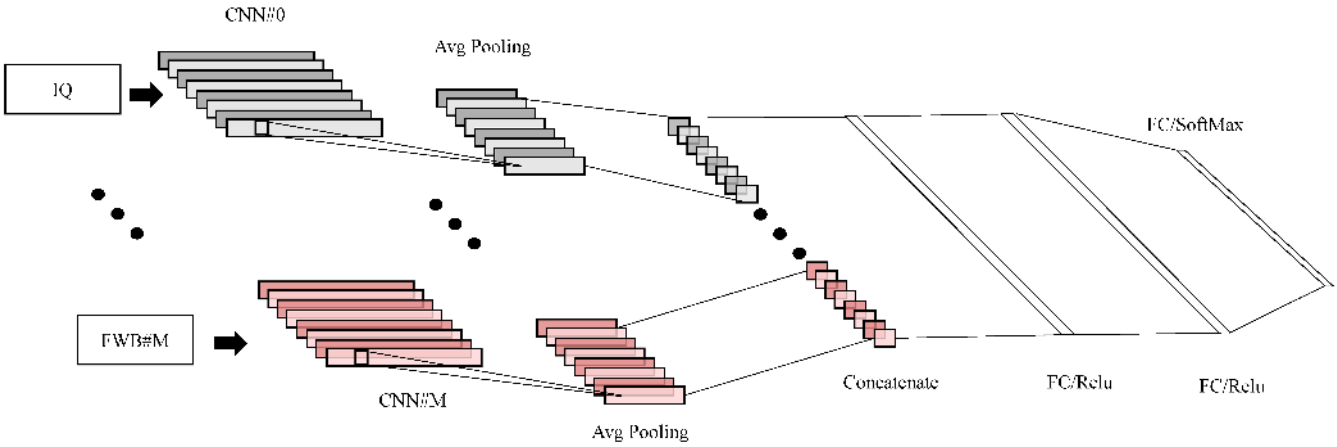

FIGURE 4. The proposed multiple input IQ and FFT Window bank (FWB) system for classifying single carrier modulation and OFDM-based wireless communication systems.

$$\hat{R}(\alpha;\tau) = \frac{1}{N_{obs}} \sum_{n=0}^{N_{obs}-1} r(n) r^*(n+\tau) e^{-j2\pi\alpha n}, \quad (4)$$

where $\hat{R}(\alpha;\tau)$ is CAF at CF α and at delay τ. N_{obs} is the observation time for calculating CAF. The estimated delay τ_m is attained by finding the local maximum of the CAF magnitude. Then, cyclostionarity test [43] is processed to check that the set of CF contains the zero ($\alpha = 0$) at delay τ_m. Therefore, the OFDM useful symbol length is estimated as $\hat{N}_{use} = \tau_m$. Rajendran [9] exploited the confusing results between LTE and DVB. We analogize the limitation of the conventional DL-base model to identify the OFDM-based technologies because of the OFDM parameter. To resolve the issue, we extend the process of the DL-base model for estimating the OFDM parameter.

B. DL-BASED BASELINE MODEL

Our baseline method leverages the CNN with IQ samples and the LSTM with the time-domain AP. The 1-dimensional transformed VGG-based CNN 8 tap model presented in [8], [38] is used as the baseline model for comparisons, and the other baseline model is the 3-layer LSTM with 128 cells [9].

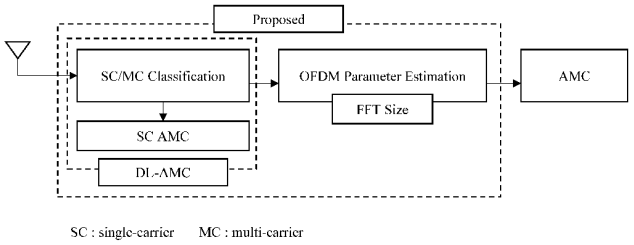

FIGURE 5. The baseline model for classifying the OFDM useful symbol length.

The input vector is L2 normalized at the amplitude vector and normalized in radians between -1 and 1 at the phase vector. The final layer of the baseline model is a softmax layer with fully connected layers (FC) in classifiers which maps the extracted features to one of the 8 output classes representing the single-carrier-based QAM and the OFDM useful symbol length.

C. PROPOSED FWB-CNN MODEL

The proposed FFT window bank (FWB)-based CNN model is used for classifying the single-carrier-based modulation and OFDM useful symbol length as shown in Fig. 3. Each

This article has been accepted for publication in a future issue of this journal, but has not been fully edited. Content may change prior to final publication. Citation information: DOI 10.1109/ACCESS.2021.3102223, IEEE Access

TABLE 1. CNN Network Layout with FWB Outputs (K is the FFT size of FWB, and M is the number of FFT processors in FWB)

ine Layer	Output dimensions	Parameter Numbers
ine Input	$2 \times K \times M$	-
Conv	$16 \times K \times M$	$M \times (1 \times 3 \times 2 + 1) \times 16$
Max Pool	$16 \times K/2 \times M$	-
Conv	$24 \times K/2 \times M$	$M \times (1 \times 3 \times 16 + 1) \times 24$
Max Pool	$24 \times K/4 \times M$	-
Conv	$32 \times K/4 \times M$	$M \times (1 \times 3 \times 24 + 1) \times 32$
Max Pool	$32 \times K/8 \times M$	-
Conv	$48 \times K/8 \times M$	$M \times (1 \times 3 \times 32 + 1) \times 48$
Max Pool	$48 \times K/16 \times M$	-
Conv	$64 \times K/16 \times M$	$M \times (1 \times 3 \times 48 + 1) \times 64$
Max Pool	$64 \times K/32 \times M$	-
Conv	$96 \times K/32 \times M$	$M \times (1 \times 3 \times 64 + 1) \times 96$
Avg. Pool	$96 \times 1 \times M$	-
FC/Relu	1024	$(M \times 96 + 1) \times 1024$
FC/Relu	1024	$1,049,600$
FC/Softmax	8	8200
ine		

FFT processor in the FWB processes the raw IQ samples with the input length N_i $(i = 1, \cdots, M)$ and a fixed FFT size K. The FFT processor requires same input and output sizes, so the input is padded with zero-valued samples when the input length is less than the FFT size. In the opposite side, the input should be truncated by the difference between the input length and FFT size. The output of ith FWB, $FWB^K_{N_i}$, is as follows:

$$FWB^K_{N_i} = \{F^K_{N_i}(0), \cdots, F^K_{N_i}(K-1)\}, (1 \leq i \leq M) \tag{5}$$

where M is the number of FWB with the FFT size K, and the output is L2 normalized to input to each CNN block. The complex sample $F^K_{N_i}(k)$ of the kth subcarrier with FFT size K using FFT window length N_i is defined as follows:

$$F^K_{N_i}(k) = \sum_{n=0}^{N_i-1} r(n) e^{-j2\pi nk/K} \tag{6}$$

where N_i represents the OFDM useful symbol length based on the transmitted sample rate before up-sampling. For instance, if the expected OFDM useful symbol length N_i is 64 and samples per symbol, O_v, is 8, the number of the input samples of the ith FFT processor is N_i extracted by the sample interval O_v from the received sample length with $N_i \times O_v$.

Each CNN block operation on each FFT output in FWB is constructed as shown in Table 1. The FWB output utilizes a single 1-D CNN to extract features, then a concatenate function is used to generate combined features before connecting it to the FC layer. The output layer adopts the ReLU function of two FC layers and the SoftMax function to map the output of the FC layers into the probabilities of the each class. Finally, the classifier predicts the OFDM useful symbol length of the received signal by selecting the class with the highest probability among the outputs of the FC/SoftMax layer.

D. PROPOSED CNN MODEL USING BOTH IQ AND FWB

The proposed FWB-CNN model can learn features for discriminating the OFDM useful symbol lengths of the received signal, and thus achieve remarkable classification accuracy performance. Furthermore, we adopt IQ signal and FWB simultaneously as input by adapting the principles of the WSMF [15] model using multimodality to improve the classification accuracy as shown in Fig. 4. The IQ sample length is the same as the FFT size of the FWB to balance the amounts of features for discriminating the single-carrier-modulation types and OFDM useful symbol lengths. By this strategy, the proposed IQ-FWB model achieves a remarkable accuracy performance to classify single-carrier-based modulation and OFDM useful symbol length at the same time.

V. DATASET GENERATION

In this section, we construct the dataset composed of an single-carrier-based modulation dataset selected from RadioML2016.10a [44] and generate an OFDM-based dataset and describe the considered wireless channel environment. We describe the organization of the trained and tested datasets.

A. MODIFIED RADIOML2016.10A

Based on RadioML2016.10a, which generated the single-carrier-based modulation dataset considered in the real environments, we selected only the modulation method used for the subcarrier in the OFDM-based wireless communication system and thus configured single-carrier modulation dataset as QPSK, 16QAM, 32QAM, and 64QAM. The modified dataset consists of 8 samples/symbol (sps), and the input sample length is configured by setting the FFT size of the FWB in the proposed system.

B. OFDM SIGNAL DATASET GENERATION WITH DIFFERENT FFT SIZE

Each wireless communication technology has a fixed OFDM useful symbol length by utilizing different FFT sizes according to the bandwidth. Assuming the same the bandwidth of all transmitted signals in this experiment, we determine the OFDM useful symbol length according to the different FFT size as 64, 128, 256, and 512. The CP ratio is fixed with 1/4. In addition, the modulation scheme used for each subcarrier of one OFDM symbol is the same, and all OFDM symbols in one frame use the same modulation scheme. Without loss of generality, the number of frames configured in the dataset consists of the same ratio of each modulation method differs with QPSK, 16QAM, 32QAM, and 64QAM as the frame index is changed.

C. DATASET CONSTRUCTION

The dataset size used to train and test the DL structure is configured as Table 2. The classification modulation scheme is composed of single-carrier-based QPSK, 16QAM, 32QAM, and 64QAM, and the modulation classification according to the OFDM useful symbol length is composed of 64-OFDM,

TABLE 2. Dataset Construction using Modified RadioML2016.10A & OFDM Dataset Parameters

ine Modulation	QPSK, 16QAM, 32QAM, 64QAM, 64-OFDM, 128-OFDM, 256-OFDM, 512-OFDM
ine Samples per Symbol	8
ine IQ Sample Length	K (FFT size of the FWB)
ine SNR Range	-10dB to +10dB (2dB step), |20|dB to |30|dB (10dB step)
ine Number of training samples	51200 frames
ine Number of test samples	51200 frames
ine	

128-OFDM, 256-OFDM, and 512-OFDM according to the FFT size. The IQ input sample length is equal to the FFT size of the FFT window bank, representing the output size of each FFT processor in FWB used as input of CNN. The sample rate is fixed at f_s, and the bandwidth is also fixed.

VI. RESULTS AND DISCUSSION

In this section, we analyze the performance of our proposed model with the parameters of FWB in AWGN, the Rayleigh fading channel, and the deviation of the LO. We discuss the limitation of the proposed model and visualize the activated neurons in the CNN according to the predicted class. In this experiment, we adopt stochastic gradient descent with momentum (SGDM) to optimize the neural network, the initial learning rate is set to 0.01, and the learning rate is reduced to 1/10 of the previous learning rate after training ten epochs. The mini-batch size is 256 in each iteration, and the proposed IQ-FWB-based CNN network is trained for 100 epochs which take around two hours of training time on an x64 i9-9900K with an Nvidia Geforce Titan Xp graphics card.

A. CLASSIFICATION RESULTS UNDER AWGN ENVIRONMENTS

We investigate the performance of conventional and proposed AMC systems under AWGN environments where only symbol timing offset exists without considering fading and frequency offset. Based on the results under the AWGN without wireless channel effects, we determine the available features to classify the single-carrier-based modulation and OFDM useful symbol length. In Fig. 6, we compare the performance of the baseline model [23], the IQ-CNN [8] with 1024 input samples, the AP-LSTM with 3 layers and 128 cells [9], proposed FWB-CNN, and IQ-FWB-CNN. The total performance of the proposed IQ-FWB-CNN is the best among the compared systems, achieving 95.8% accuracy at high SNR ranges except the baseline model with 97.6% accuracy. The baseline model requires longer observation period than DL-model to achieve satisfactory performance. The conventional AMC systems achieve 62.8% using IQ-CNN and 61.8% using AP-LSTM. The proposed FWB-CNN achieves 58.5%, which is the lowest accuracy among the compared systems.

In order to examine the classification performance in detail, we calculated the confusion matrix of each AMC system under the AWGN channel at an SNR of 20 dB as shown in Figs. 7 and 8. In Fig. 7, the conventional AMC systems do not cause confusion between single-carrier and multi-carrier, and the performance of classifying single-carrier modulation is very high with 99.8%. However, the performance of classifying signals with different OFDM useful symbol lengths is very low with 24.1%, representing that the system is confusing to discriminate. On the other hand, in Fig. 8, the proposed FWB-CNN system achieves an accuracy of 98.2% for classifying different OFDM useful symbol lengths, but the accuracy of single carrier-based modulation classification is very low with 18.2%. Therefore, the proposed IQ-FWB-CNN achieves the highest accuracy performance compared with IQ, AP, and FWB feature-based DL structure for classifying single-carrier-based modulation and the OFDM useful

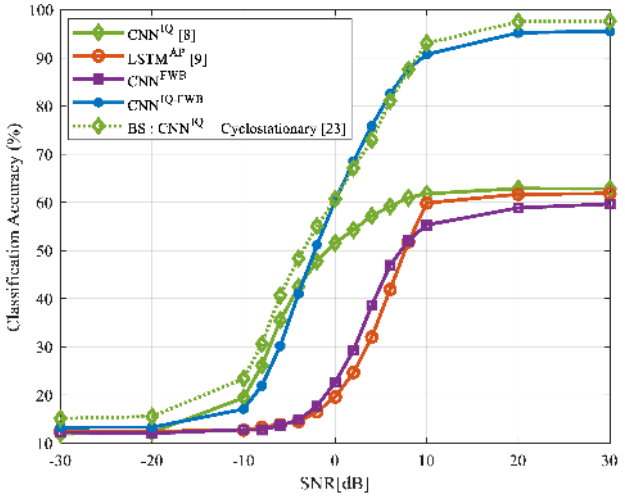

FIGURE 6. The accuracy performance results for classifying single-carrier-based modulation and OFDM useful symbol length under AWGN channel with baseline model, conventional DL model, proposed FWB-CNN, and IQ-FWB-CNN model.

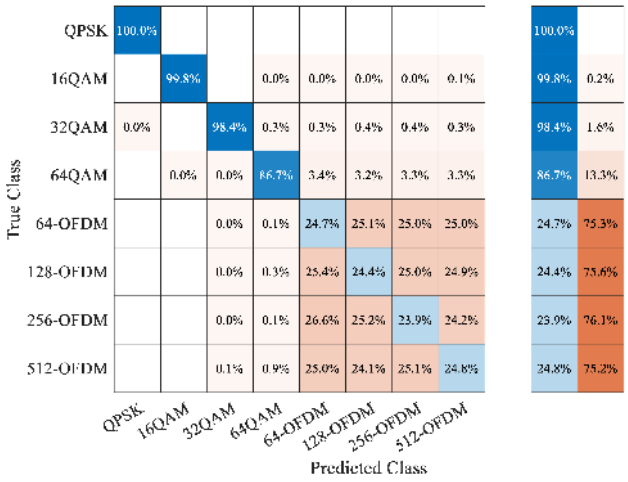

FIGURE 7. The confusion matrix for classifying single-carrier-based modulation and OFDM useful symbol length in conventional DL structure under AWGN channel at an SNR of 20 dB.

This article has been accepted for publication in a future issue of this journal, but has not been fully edited. Content may change prior to final publication. Citation information: DOI 10.1109/ACCESS.2021.3102223, IEEE Access

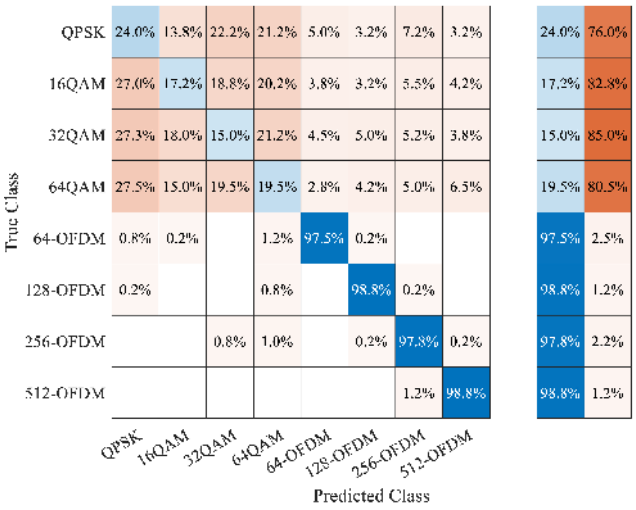

FIGURE 8. The confusion matrix for classifying single-carrier-based modulation and OFDM useful symbol length in proposed FWB-CNN structure composed of 64, 128, 256, 512 length with 1024 FFT size under AWGN channel at an SNR of 20 dB.

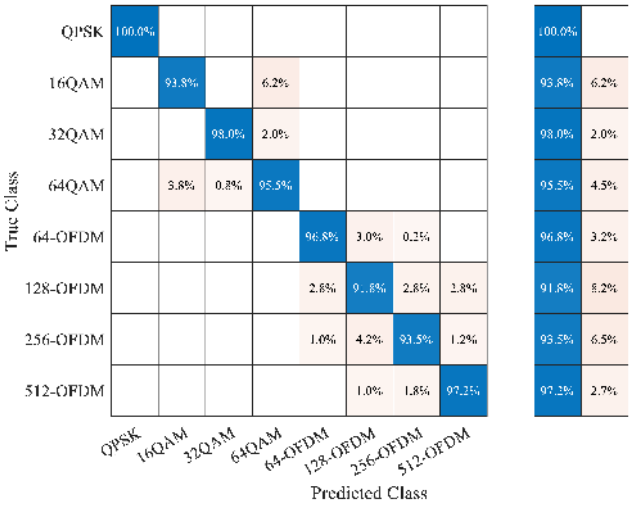

FIGURE 9. The confusion matrix for classifying SC modulation and OFDM useful symbol length in proposed IQ-FWB-CNN structure composed of 64, 128, 256, 512 length with 1024 FFT size under AWGN channel at an SNR of 20 dB.

symbol length at the same time as shown in Fig. 9. However, at low SNR ranges, the classification accuracy of IQ-CNN is higher than that of IQ-FWB-CNN. The IQ-FWB-CNN utilizes both IQ and the FWB features at the same time. Since the accuracy of FWB-CNN is very low below SNR -6 dB, the accuracy of IQ-FWB-CNN is lower than the IQ-CNN.

The proposed IQ-FWB-CNN method jointly and simultaneously classifies the modulation schemes and the OFDM useful symbol length by adding the FWB feature to the conventional IQ-CNN. The conventional IQ-CNN confused to classify 64QAM and OFDM signal as shown in Fig. 7, but the additional FWB features of the OFDM useful symbol length reduce the false classification case as shown in Fig. 9. Therefore, the classification of the OFDM useful symbol

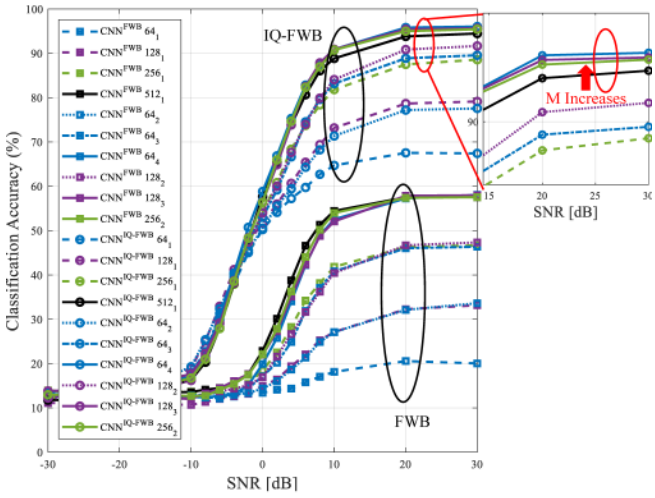

FIGURE 10. The accuracy performance for classifying single-carrier-based modulation and OFDM useful symbol length of the proposed IQ-FWB-CNN structure as the FWB maximum FFT window length and the number of FWB increase.

length helps with the classification of modulation schemes.

The conventional AMC methods using FFT magnitude achieved satisfactory performance on modulation classification [15]. However, the proposed FWB-based model aims to extract features of OFDM useful symbol length. Thus, the extraction of input on FFT processors is different from the conventional methods. The conventional input follows the sampling rate of the receiver, but the FWB pre-processor extracts the input samples of FFT processors by re-sampling the received sample with the expected inverse FFT (IFFT) size over the expected OFDM useful symbol length. Thus, the output of the FWB results in the loss of information in the case of single-carrier signals, resulting in poor classification performance compared to the conventional AMC methods using the FFT magnitude.

To acquire the classification accuracy as shown in Fig. 6, the FWB of the proposed model consists of four FFT processors with an FFT size of 1024 and FFT window lengths of 64, 128, 256, and 512, respectively. The FFT window bank is constructed based on the OFDM useful symbol length of the dataset, and thus we expect to acquire the highest performance compared to other methods. However, we cannot determine the OFDM useful symbol length in real environments since the receiver does not know the transmitted OFDM useful symbol length. To address the issue, we try to find the constraints of the FWB parameter to obtain reasonable classification accuracy in the following subsection.

B. PERFORMANCE CONSTRAINTS OF FWB PARAMETERS

We analyze the classification accuracy performance according to the number and window length of FFT processors in FWB using a fixed FFT size of 1024 as shown in Fig. 10. CNN N_M shown in Fig. 10 represents the classification accuracy of a CNN model using FWB consisting of M FFT

This article has been accepted for publication in a future issue of this journal, but has not been fully edited. Content may change prior to final publication. Citation information: DOI 10.1109/ACCESS.2021.3102223, IEEE Access

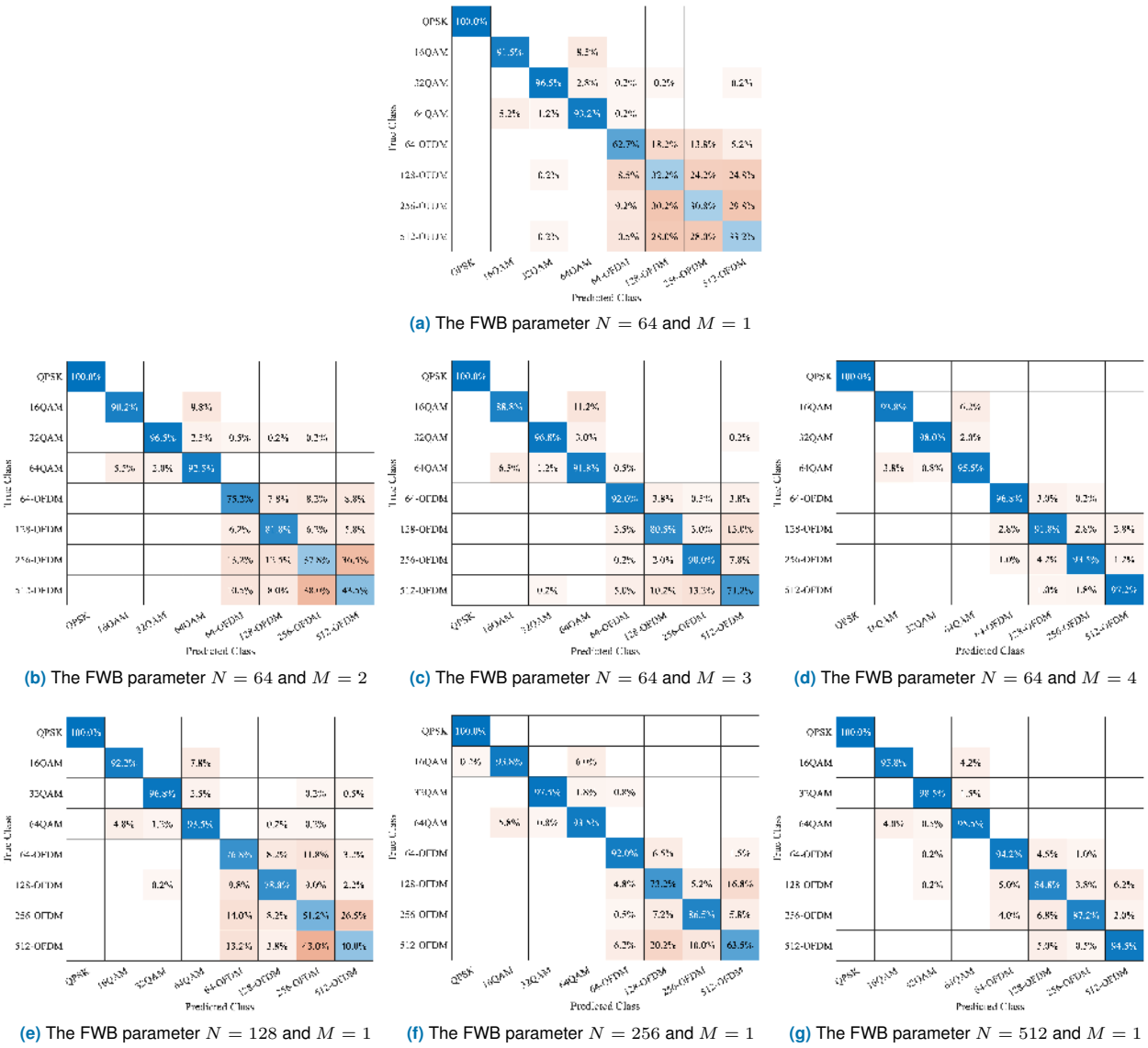

(a) The FWB parameter $N = 64$ and $M = 1$

(b) The FWB parameter $N = 64$ and $M = 2$

(c) The FWB parameter $N = 64$ and $M = 3$

(d) The FWB parameter $N = 64$ and $M = 4$

(e) The FWB parameter $N = 128$ and $M = 1$

(f) The FWB parameter $N = 256$ and $M = 1$

(g) The FWB parameter $N = 512$ and $M = 1$

FIGURE 11. The confusion matrix of the proposed IQ-FWB-CNN to find the effects of the FWB maximum FFT length for classifying different OFDM useful symbol lengths under AWGN channel with an SNR of 20 dB.

processors with an FFT window length of $N_i = N \times 2^{i-1}$ $(1 \leq i \leq M)$. Based on the result, the proposed FWB-CNN confused the OFDM signals with the different lengths when the maximum FFT window length (N_M) in FWB is shorter than the maximum OFDM useful symbol length of the dataset. In the opposite case, the performance of the proposed system achieves the highest accuracy performance for classifying the OFDM useful symbol length.

In Fig. 11, the confusion matrix shows the classification performance of the proposed IQ-FWB-CNN for different OFDM useful symbol lengths according to the maximum FFT window length in FWB under the AWGN channel with an SNR of 20 dB. The shortest FFT window length 64 of the FWB classifies only the OFDM signal with the FFT size 64 (64-OFDM) among the transmitted OFDM signal with different lengths as shown in Fig. 11(a). From Figs. 11(b) to 11(d), the classification results shows that the classified OFDM useful symbol length increases as larger the number of FFT processors in FWB using the starting FFT window length (N_1) of 64. To find the effect of the only maximum FFT window length, we obtain the confusion matrix as the starting FFT window length increases as shown in from Figs. 11(e) to 11(g). Based on the results, we should select the maximum FFT window length in FWB longer than the classifying OFDM useful symbol length to achieve reasonable classification accuracy. In Fig. 10, the classification accuracy performance improves as the larger the number of FWB even though the maximum FFT window length is the same.

We also analyzed the classification accuracy performance to explore the effect of FFT size, the other parameter of FWB as shown in Fig. 12. The classification performance achieves over 90% accuracy when the FFT size of the FWB is larger

This article has been accepted for publication in a future issue of this journal, but has not been fully edited. Content may change prior to final publication. Citation information: DOI 10.1109/ACCESS.2021.3102223, IEEE Access

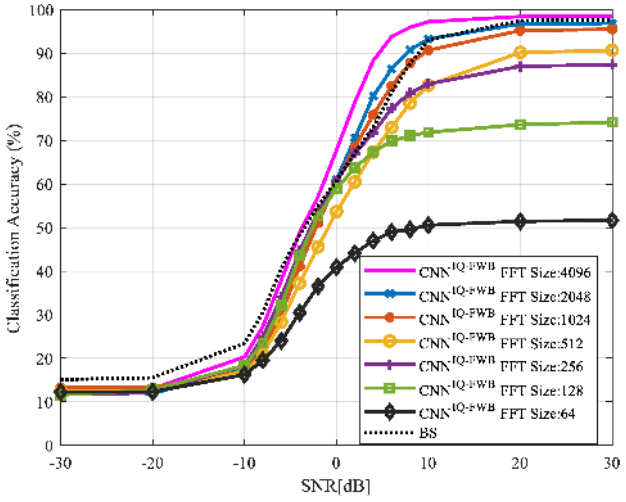

FIGURE 12. The classification accuracy performance of the proposed IQ-FWB-CNN structure as the FFT size increases under AWGN channel.

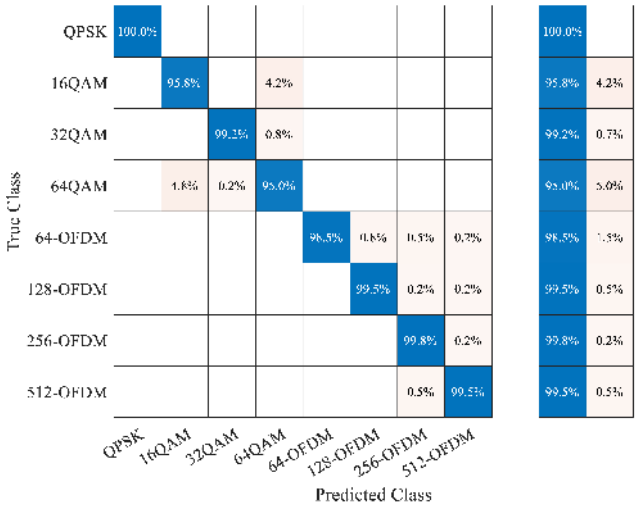

FIGURE 13. The confusion matrix of the proposed IQ-FWB-CNN structure with the FFT size 4096 under AWGN channel with an SNR of 20 dB.

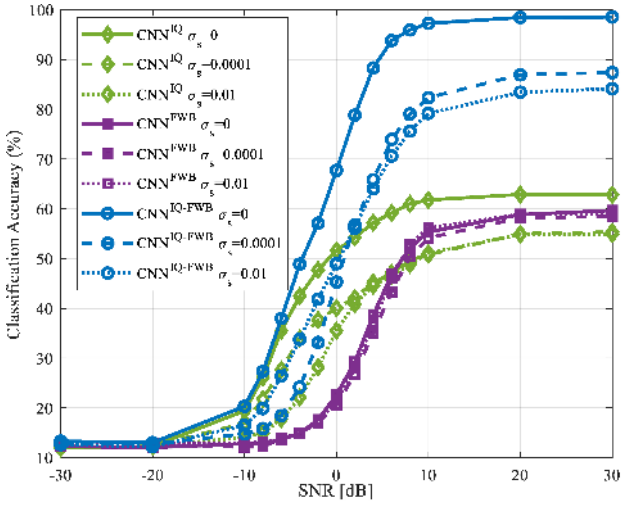

FIGURE 14. The classification accuracy performance of the proposed FWB-CNN and IQ-FWB-CNN under AWGN channel with synchronization offset $\sigma_s = 0.0001$ and $\sigma_s = 0.01$.

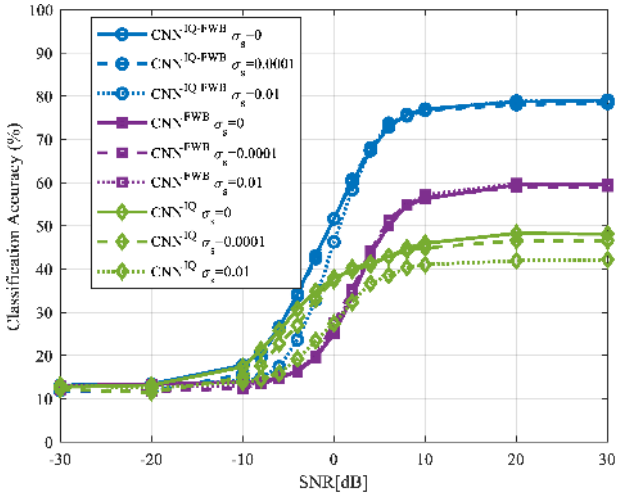

FIGURE 15. The classification accuracy performance of the proposed FWB-CNN and IQ-FWB-CNN under 3-tap modeled Rayleigh Fading channel with synchronization offset $\sigma_s = 0.0001$ and $\sigma_s = 0.01$.

than that of the transmitted OFDM signal, which is similar to the trend obtained from the maximum FFT window length. Based on the results, the proposed IQ-FWB-CNN model achieves the higher performance of 98.5% than the baseline model of 97.6% at high SNR ranges when the FFT size of the FWB is 4096 as shown in Fig. 13, and thus we fixed the FFT size of the proposed model at 4096 in the following experiments.

C. CLASSIFICATION UNDER FADING CHANNEL WITH SYNCHRONIZATION OFFSET

In real environments, the LO of transmitter and receiver is compensated by estimating the synchronization offset, which distorts the received signal. To analyze the classification performance of the proposed system according to synchronization offset effects as shown in Fig. 14, we adopt the frequency offset variance σ_s of carrier and sampling in two cases as minor LO offset with $\sigma_s = 0.0001$ and moderate LO offset with $\sigma_s = 0.01$. Under the mismatched LO frequency offset, the IQ-FWB-CNN performance degrades 87.3% in a minor offset case and 83.4% in the moderate offset case from 98.5% without offset at high SNR ranges. Furthermore, the IQ-CNN performance degrades from 62.8% in the no offset case to 54.9% in the minor/moderate offset case. Since the FWB-CNN performance is the same as 59.6% in no-offset cases even the LO offset increases, the degradation of IQ-FWB-CNN performance comes from the IQ sample input.

We modeled the Rayleigh fading channel with 3-tap FIR filter consists of $\tau = 1.8$ with -2 dB gain and $\tau = 3.4$ with -10 dB gain to obtain the accuracy performance of the classifiers. In Fig. 15, the proposed IQ-FWB-CNN performance achieves the classification accuracy of 78.9% constantly even

This article has been accepted for publication in a future issue of this journal, but has not been fully edited. Content may change prior to final publication. Citation information: DOI 10.1109/ACCESS.2021.3102223, IEEE Access

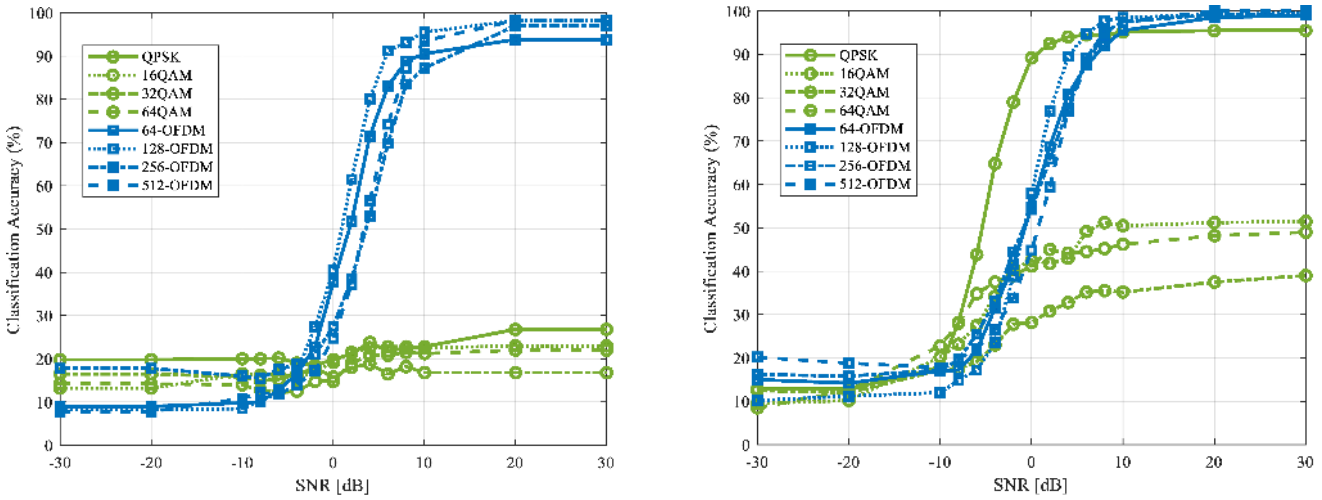

(a) The FWB-CNN with the FWB parameters 64_4 and 4096 FFT size

(b) The IQ-FWB-CNN with the FWB parameters 64_4 and 4096 FFT size

FIGURE 16. The each modulation classification accuracy performance of the proposed FWB-CNN and IQ-FWB-CNN under 3-tap modeled Rayleigh Fading channel with synchronization offset $\sigma_s = 0.01$

the deviation of the synchronization offset increases. The IQ-CNN classification accuracy is 48.2% without synchronization offset, 46.5% at a minor offset, and 42.1% at moderate offset under the Rayleigh fading channel. However, the FWB-CNN performance is constant with 59.6% as the same as the performance of the AWGN channel, which the distortion of the signals does not affect the accuracy performance for classifying different OFDM useful symbol lengths.

Based on those results and the performance shown in Fig. 16(a), the CNN using FWB extracts the classification features robust to the distortion of the transmitted signal by the fading and synchronization offset. In Fig. 16(b), the IQ-FWB-CNN performance for different OFDM useful symbol lengths and QPSK achieves high accuracy of 99.8% at high SNR ranges under Rayleigh fading channels with the moderate LO offset. On the other hand, the classification accuracy of QAM-based modulation degrades 51.5% at 16-QAM, 49.0% at 32-QAM, and 39.1% at 64-QAM by the effect of the fading channel.

D. DISCUSSION ABOUT THE LIMITATION OF THE PROPOSED IQ-FWB-CNN

We investigated the constraints of FWB prameters to acquire the improved performance in the previous subsections. When the FFT window length is shorter than the OFDM useful symbol length to be classified by performing according to the OFDM useful symbol length and the number of banks, the signal classification performance is deficient. However, when the FFT input length is longer than the OFDM useful symbol length, the classification performance is high. Therefore, classification is possible only by setting the FFT window length longer than the OFDM useful symbol length. For this reason, the fact that the modulation method can be classified with a short sample input length, which is an advantage of the conventional DL-based AMC system, becomes impossible by using the FFT window bank.

We find the cause of this phenomenon by using a classification activation map (CAM) [45] to visualize the image positions activated by the CNN. Since the referenced approach is based on image, we change it to a signal-based method. Even with the same OFDM useful symbol length, the CAM regions are different from each other since each frame has randomized information. Therefore, we analyzed the average CAM regions for each OFDM useful symbol length type for every frame tested as shown in Fig. 17. Using 4 FFT banks, we can see that the responding FFT bank varies according to the transmitted OFDM useful symbol length as shown in Fig. 17(a). By using one FFT bank, when the received signal is 64 FFT sized OFDM signals, Fig. 17(b) shows the equal response to all subcarriers, and the received signals with the OFDM useful symbol length of 256 and 512 show a smaller response as it moves away from the center. At 128, the reaction occurs more strongly in the time-domain IQ samples than in the FWB. Those results show that CNN classifies OFDM useful symbol length types better as the number of banks increases. However, based on these results, we cannot clarify why the FFT parameters are limited to values with a longer input length and a larger FFT size than the transmitted OFDM signal.

The OFDM signal has the same modulation scheme used for each subcarrier. The method of classifying these modulation schemes was possible through the CNN [42] structure using the input of the time-domain IQ signal. When the FFT window bank proposed in this paper is applied, several OFDM symbols are overlapped as one FFT output, so there is a limitation in classifying the modulation scheme used for each subcarrier. Fig. 18 shows the limitation that the proposed system confuses on modulation schemes used in the OFDM subcarrier even though the system classifies the

This article has been accepted for publication in a future issue of this journal, but has not been fully edited. Content may change prior to final publication. Citation information: DOI 10.1109/ACCESS.2021.3102223, IEEE Access

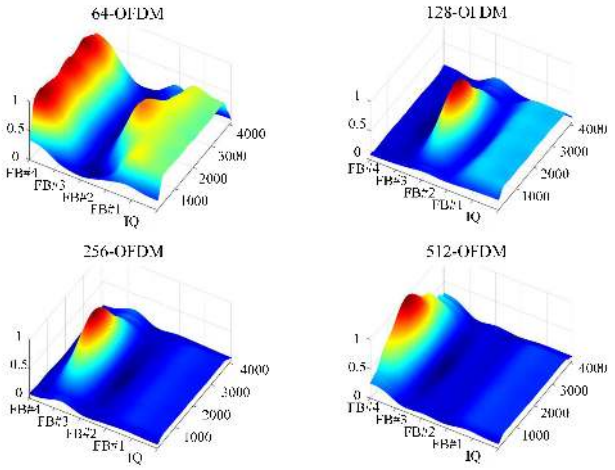

(a) The IQ-FWB-CNN with the FWB parameters 64_4 and 4096 FFT size

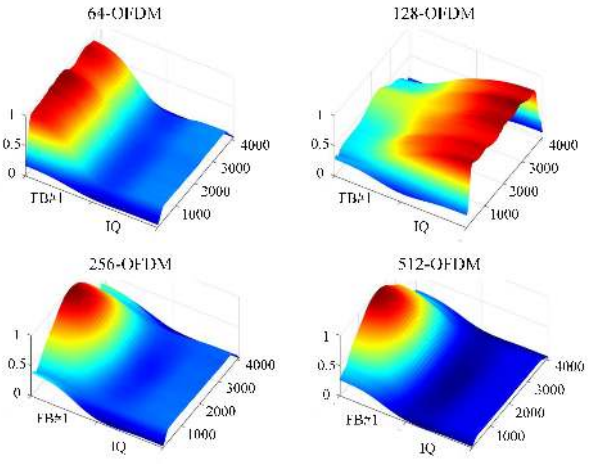

(b) The IQ-FWB-CNN with the FWB parameters 512_1 and 4096 FFT size

FIGURE 17. The CNN activation visualization using classification activation map (CAM) under AWGN channel at an SNR of 20 dB.

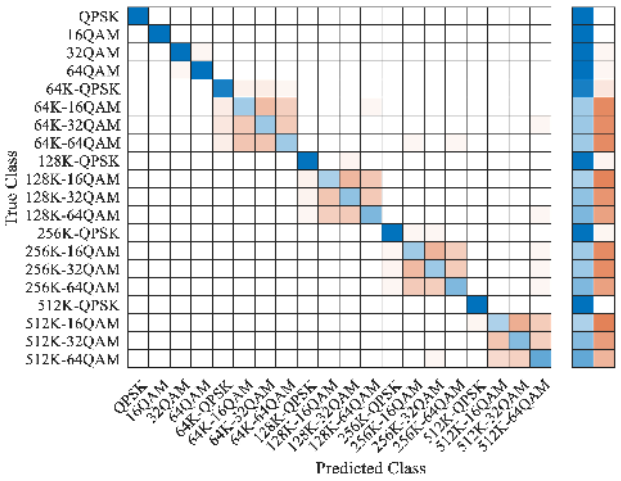

FIGURE 18. The confusion matrix of the proposed IQ-FWB CNN under AWGN channel at an SNR of 20 dB.

single-carrier modulation scheme and OFDM useful symbol length.

We analyzed the complexity of the multiple FFT processors [46] in FWB and the floating-point operations (FLOPs) of the DL-based model [47] as shown in Table. 3. The input sample length of IQ-CNN, FWB-CNN, and IQ-FWB-CNN is the FFT size 4096 of the FWB, and the number of FFT processors on FWB is four. The number of LSTM cells is 128, and the depth of the LSTM layer is three. The conventional IQ-CNN model has about 1.19×10^6 parameters, and the uncompressed size is at least $1,193,216 \times 32$ bits/float $\approx$ 381MB. AP-LSTM has about 0.33×10^6 parameters, and the uncompressed size is at least $331,272 \times 32$ bits/float $\approx$ 10MB. FWB-CNN model has about 1.59×10^6 parameters, and the uncompressed size is at least $1,596,392 \times 32$ bits/float $\approx$ 51MB. IQ-FWB-CNN model has about 1.63×10^6 parameters, and the uncompressed size is at least

TABLE 3. The numbers of parameters and FLOPs of the several algorithms ($K = 4096, M = 4$)

ine model	params	FLOPs
ine IQ-CNN	1.19×10^6	27.09×10^6
ine AP-LSTM	0.33×10^6	9.51×10^6
ine FWB-CNN	1.59×10^6	102.02×10^6
ine IQ-FWB-CNN	1.63×10^6	127.00×10^6
ine FFT Processors in FWB ine	-	0.983×10^6

$1,632,480 \times 32$ bits/float $\approx$ 52MB. The proposed IQ-FWB-CNN model gives $\times 1.33$ and $\times 4.68$ (IQ-CNN) increases in total parameters and FLOPs respectively. The FLOPs of FFT processors add to the total FLOPs of IQ-FWB-CNN with $983,040$. Thus, the complexity of the proposed IQ-FWB-CNN model is too high to implement on the low-cost spectrum sensors.

VII. CONCLUSION

In this paper, we proposed an FFT window bank consisted of several different FFT window lengths and fixed FFT size and the CNN model operating on IQ and FWB simultaneously to improve the classification accuracy for identifying the OFDM-based signal such as LTE, DVB, WLAN, and 5G, which the prior works have confused. We also have conducted performance evaluations in AWGN, fading, and synchronization offset environments. We have found the constraints of the FWB parameters to achieve reasonable classification accuracy by analyzing the performance, and we tried to find the cause of the constraints by visualizing the classification activation map. Furthermore, we have discussed the disadvantages of the proposed model compared to the conventional methods, which the proposed model required longer input sample length trade-offs of different OFDM useful symbol lengths classification than the advantage of

short input sample in conventional methods with confusing OFDM-based signals.

We still have much to overcome the limitation of the proposed system by acquiring features of OFDM-based signal with shorter input length adapting other DL structure. In this work, the guard interval and the bandwidth of the transmitted OFDM signals is fixed and the same unlike the real wireless communication signals, and the guard interval estimation is required to implement in the real world. Furthermore, the performance evaluation is required under the unseen channel environments such as multi-input multi-output system, vehicle-to-everything (V2X) and other complex environments.

REFERENCES

[1] W. Gardner, "Signal interception: A unifying theoretical framework for feature detection," *IEEE Trans. Commun.*, vol. 36, no. 8, pp. 897–906, 1988.

[2] W. Gardner, "Spectral correlation of modulated signals: Part I - Analog modulation," *IEEE Trans. Commun.*, vol. 35, no. 6, pp. 584–594, Jun. 1987.

[3] W. Gardner, W. Brown, and C.-K. Chen, "Spectral correlation of modulated signals: Part II - Digital modulation," *IEEE Trans. Commun.*, vol. 35, no. 6, pp. 595–601, Jun. 1987.

[4] A. Nandi and E. Azzouz, "Algorithms for automatic modulation recognition of communication signals," *IEEE Trans. Commun.*, vol. 46, no. 4, pp. 431–436, 1998.

[5] O. Dobre, A. Abdi, Y. Bar-Ness, and W. Su, "Survey of automatic modulation classification techniques: Classical approaches and new trends," *IET Commun.*, vol. 1, no. 2, pp. 137–156, April 2007.

[6] B. Kroon, S. Bergin, I. O. Kennedy, and G. O'Mahony Zamora, "Steady state RF fingerprinting for identity verification: One class classifier versus customized ensemble," in *Proc. Artif. Intell. Cogn. Sci.*, 2010, pp. 198–206.

[7] K. Youssef, L. Bouchard, K. Haigh, J. Silovsky, B. Thapa, and C. V. Valk, "Machine learning approach to RF transmitter identification," *IEEE J. Radio Freq. Identificat.*, vol. 2, no. 4, pp. 197–205, Dec. 2018.

[8] T. J. O'Shea, T. Roy, and T. C. Clancy, "Over-the-air deep learning based radio signal classification," *IEEE J. Sel. Topics Signal Process.*, vol. 12, no. 1, pp. 168–179, Feb. 2018.

[9] S. Rajendran, W. Meert, D. Giustiniano, V. Lenders, and S. Pollin, "Deep learning models for wireless signal classification with distributed low-cost spectrum sensors," *IEEE Trans. on Cogn. Commun. Netw.*, vol. 4, no. 3, pp. 433–445, Sept. 2018.

[10] N. E. West and T. O'Shea, "Deep architectures for modulation recognition," in *Proc. IEEE Int. Symp. Dyn. Spectr. Access Netw. (DySPAN)*, Piscataway, NJ, USA, Mar. 2017, pp. 1–6.

[11] S. Peng, H. Jiang, H. Wang, H. Alwageed, Y. Zhou, M. M. Sebdani, and Y.-D. Yao, "Modulation classification based on signal constellation diagrams and deep learning," *IEEE Trans. Neural Netw. Learn. Syst.*, vol. 30, no. 3, pp. 718–727, Mar. 2019.

[12] A. Krizhevsky, I. Sutskever, and G. E. Hinton, "ImageNet classification with deep convolutional neural networks," in *Proc. Adv. Neural Inf. Process. Syst.*, vol. 25, 2012, pp. 1097–1105.

[13] C. Szegedy, W. Liu, Y. Jia, P. Sermanet, S. Reed, D. Anguelov, D. Erhan, V. Vanhoucke, and A. Rabinovich, "Going deeper with convolutions," in *Proc. IEEE Conf. Comput. Vis. Pattern Recognit. (CVPR)*, Jun. 2015. [Online]. Available: http://arxiv.org/abs/1409.4842

[14] Y. Zhou, T. Lin, and Y. Zhu, "Automatic modulation classification in time-varying channels based on deep learning," *IEEE Access*, vol. 8, pp. 197 508–197 522, Oct. 2020.

[15] P. Qi, X. Zhou, S. Zheng, and Z. Li, "Automatic modulation classification based on deep residual networks with multimodal information," *IEEE Trans. on Cogn. Commun. Netw.*, vol. 7, no. 1, pp. 21–33, Mar. 2021.

[16] S. Rajendran, R. Calvo-Palomino, M. Fuchs, B. Van den Bergh, H. Cordobes, D. Giustiniano, S. Pollin, and V. Lenders, "Electrosense: Open and big spectrum data," *IEEE Commun. Mag.*, vol. 56, no. 1, pp. 210–217, Jan. 2018.

[17] J. L. Xu, W. Su, and M. Zhou, "Likelihood-ratio approaches to automatic modulation classification," *IEEE Trans. Syst., Man, Cybern. C*, vol. 41, no. 4, pp. 455–469, July 2011.

[18] W. Xie, S. Hu, C. Yu, P. Zhu, X. Peng, and J. Ouyang, "Deep learning in digital modulation recognition using high order cumulants," *IEEE Access*, vol. 7, pp. 63 760–63 766, 2019.

[19] B. Kim, J. Kim, H. Chae, D. Yoon, and J. W. Choi, "Deep neural network-based automatic modulation classification technique," in *Proc. Int. Conf. Inf. Commun. Technol. Converg. (ICTC)*, Oct. 2016, pp. 579–582.

[20] J. Lee, B. Kim, J. Kim, D. Yoon, and J. W. Choi, "Deep neural network-based blind modulation classification for fading channels," in *Proc. Int. Conf. Inf. Commun. Technol. Convergence*, Oct. 2017, pp. 551–554.

[21] S. Hu, Y. Pei, P. P. Liang, and Y. Liang, "Deep neural network for robust modulation classification under uncertain noise conditions," *IEEE Trans. Veh. Technol.*, vol. 69, no. 1, pp. 564–577, Jan. 2020.

[22] T. Yucek and H. Arslan, "OFDM signal identification and transmission parameter estimation for cognitive radio applications," in *Proc. IEEE GLOBECOM*, Dec. 2007, pp. 4056–4060.

[23] A. Punchihewa, V. K. Bhargava, and C. Despins, "Blind Estimation of OFDM parameters in Cognitive Radio Networks," *IEEE Trans. Wireless Commun.*, vol. 10, no. 3, pp. 733–738, 2011.

[24] A. Bouzegzi, P. Ciblat, and P. Jallon, "New algorithms for blind recognition of OFDM based systems," *Signal Processing*, vol. 90, no. 3, pp. 900–913, 2010.

[25] R. Heath and G. Giannakis, "Exploiting input cyclostationarity for blind channel identification in OFDM systems," *IEEE Trans. Signal Process.*, vol. 47, no. 3, pp. 848–856, Mar. 1999.

[26] H. Ishii and G. W. Wornell, "OFDM blind parameter identification in cognitive radios," in *Proc. IEEE Int. Symp. Pers. Indoor Mobile Radio Commun. (PIMRC)*, vol. 1, Sept. 2005, pp. 700–705.

[27] F. Gini and G. Giannakis, "Frequency offset and symbol timing recovery in flat-fading channels: a cyclostationary approach," *IEEE Trans. Commun.*, vol. 46, no. 3, pp. 400–411, Mar. 1998.

[28] Y. Yao and G. Giannakis, "Blind carrier frequency offset estimation in SISO, MIMO, and multiuser OFDM systems," *IEEE Trans. Commun.*, vol. 53, no. 1, pp. 173–183, Jan. 2005.

[29] H. Bolcskei, "Blind estimation of symbol timing and carrier frequency offset in wireless OFDM systems," *IEEE Trans. Commun.*, vol. 49, no. 6, pp. 988–999, Jun 2001.

[30] N. E. West and T. O'Shea, "Convolutional radio modulation recognition networks," in *Proc. Int. Conf. Eng. Appl. Neural Netw.*, 2016, pp. 213–226.

[31] K. Simonyan and A. Zisserman, "Very deep convolutional networks for large-scale image recognition," arXiv:1409.1556, 2014.

[32] C.-F. Teng, C.-Y. Chou, C.-H. Chen, and A.-Y. Wu, "Accumulated polar feature-based deep learning for efficient and lightweight automatic modulation classification with channel compensation mechanism," *IEEE Trans. Veh. Technol.*, vol. 69, no. 12, pp. 15 472–15 485, Dec. 2020.

[33] F. Meng, P. Chen, L. Wu, and X. Wang, "Automatic modulation classification: A deep learning enabled approach," *IEEE Trans. Veh. Technol.*, vol. 67, no. 11, pp. 10 760–10 772, Nov. 2018.

[34] K. Yashashwi, A. Sethi, and P. Chaporkar, "A learnable distortion correction module for modulation recognition," *IEEE Wireless Commun. Lett.*, vol. 8, no. 1, pp. 77–80, Feb. 2019.

[35] S. Chen, Y. Zhang, Z. He, J. Nie, and W. Zhang, "A novel attention cooperative framework for automatic modulation recognition," *IEEE Access*, vol. 8, pp. 15 673–15 686, 2020.

[36] M. Kulin, T. Kazaz, I. Moerman, and E. De Poorter, "End-to-end learning from spectrum data: A deep learning approach for wireless signal identification in spectrum monitoring applications," *IEEE Access*, vol. 6, pp. 18 484–18 501, 2018.

[37] R. Zhou, F. Liu, and C. W. Gravelle, "Deep learning for modulation recognition: A survey with a demonstration," *IEEE Access*, vol. 8, pp. 67 366–67 376, 2020.

[38] *Modulation Classification With Deep Learning*. Mathworks, Natick, MA, USA, 2019.

[39] Y. Wang, M. Liu, J. Yang, and G. Gui, "Data-driven deep learning for automatic modulation recognition in cognitive radios," *IEEE Trans. Veh. Technol.*, vol. 68, no. 4, pp. 4074–4077, Apr. 2019.

[40] G. J. Mendis, J. Wei-Kocsis, and A. Madanayake, "Deep learning based radio-signal identification with hardware design," *IEEE Trans. Aerosp. Electron. Syst.*, vol. 55, no. 5, pp. 2516–2531, Oct. 2019.

[41] Q. Cheng, Z. Shi, D. N. Nguyen, and E. Dutkiewicz, "Sensing ofdm signal: A deep learning approach," *IEEE Trans. Commun.*, vol. 67, no. 11, pp. 7785–7798, 2019.

[42] S. Hong, Y. Zhang, Y. Wang, H. Gu, G. Gui, and H. Sari, "Deep learning-based signal modulation identification in OFDM systems," *IEEE Access*, vol. 7, pp. 114 631–114 638, 2019.

[43] A. Dandawate and G. Giannakis, "Statistical tests for presence of cyclostationarity," *IEEE Trans. Signal Process.*, vol. 42, no. 9, pp. 2355–2369, 1994.
[44] T. O'Shea and N. West, "Radio machine learning dataset generation with GNU radio," *Proc. GNU Radio Conf*, vol. 1, no. 1, 2016.
[45] B. Zhou, A. Khosla, A. Lapedriza, A. Oliva, and A. Torralba, "Learning deep features for discriminative localization," in *Proc. IEEE Conf. Comput. Vis. Pattern Recognit.(CVPR)*, Jun 2016, pp. 2921–2929.
[46] *Inside the FFT Black Box Serial and Parallel Fast Fourier Transform Algorithms*. CRC New York, 2019.
[47] M. Thoma, "Analysis and optimization of convolutional neural network architectures," Masters's Thesis, Karlsruhe Institute of Technology, Karlsruhe, Germany, Jun. 2017. [Online]. Available: https://martin-thoma.com/msthesis/

MYUNG CHUL PARK received his B.S. and M.S. degrees from Kypungpook National University, Daegu, Korea, in 2013 and 2015, respectively. He is currently pursuing his Ph.D. degree. His main research interests are wireless communication system and automatic modulation constellation.

DONG SEOG HAN received the B.S. degree in electronic engineering from Kyungpook National University (KNU), Daegu, South Korea, in 1987, and the M.S. and Ph.D. degrees in electrical engineering from the Korea Advanced Institute of Science and Technology, Daejon, South Korea, in 1989 and 1993, respectively. From 1987 to 1996, he was with Samsung Electronics Co., Ltd., where he developed the transmission systems for QAM HDTV and Grand Alliance HDTV receivers. Since 1996, he has been with the School of Electronics Engineering, KNU, as a Professor. He was a courtesy Associate Professor with the Department of Electrical and Computer Engineering, University of Florida, in 2004. He was the Director with the Center of Digital TV and Broadcasting, Institute for Information Technology Advancement, from 2006 to 2008. His main research interests include intelligent signal processing and autonomous vehicles.